

# Dielectric and Calorimetric Behaviors of Poly(vinyl methyl ether)–Water Systems Including Unusual Relaxation Processes at Subzero Temperatures

Hideatsu Maeda

National Institute for Advanced Interdisciplinary Research and National Institute of Bioscience and Human-technology, 1-1-4 Higashi, Tsukuba, Ibaraki 305, Japan

Received January 9, 1995

Revised Manuscript Received April 27, 1995

**(1) Introduction.** The thermal behavior of macromolecular aqueous solutions at subzero temperatures has been studied. In particular, calorimetric studies on a series of thermal transitions occurring in solution (nucleation and crystallization on cooling; glass transition, recrystallization, and eutectic melting on warming) have been made for several polymers.<sup>1–7</sup>

In order to get information regarding the dynamics of macromolecular aqueous solutions at subzero temperatures, we have carried out complex dielectric experiments together with calorimetric and optical microscopic measurements for poly(vinyl methyl ether) (PVME)–water systems.

Poly(vinyl methyl ether) is a water-soluble polymer that undergoes a phase transition at approximately 35 °C (the cloud-point temperature).<sup>8</sup> We have recently found two critical polymer concentrations in PVME–water systems that suggest two distinct hydrogen-bonded water structures on each polymer chain.<sup>9</sup>

With the above three methods, we have determined six characteristic temperature regions in PVME (more than 40%)–water systems and three characteristic regions in the PVME (less than 40%)–water systems at temperatures between –150 and 0 °C. The following marked dielectric behaviors have been found: (i) a drastic change in relaxation times of water between lower and higher temperature boundaries of the glass transition region around –80 °C, (ii) two sharp reductions (at –66 and –24 °C) in the dielectric constant due to different types of recrystallization of water, and (iii) an unusual relaxation process in which the relaxation times become longer (slow down) with increasing temperature above –20 °C. Calorimetrically, we have found two critical polymer concentrations below 0 °C, which are in good agreement with those determined from DSC data around 36 °C in a previous paper.<sup>9</sup>

**(2) Experimental Section.** Poly(vinyl methyl ether) was obtained as a 50% aqueous solution from the Aldrich Chemical Co., Inc.

A capacitance bridge (General Radio 1616) was used for the complex dielectric measurements. In addition, calorimetric measurements (Mettler 30 and Perkin Elmer DSC 7 calorimeters) were carried out using a scanning rate of 3 °C/min. The weight of samples sealed in aluminum pans was approximately 10 mg. Morphologies of PVME–water systems were investigated between –100 and 0 °C by an optical microscope with a cooling stage (Japan Hitech Th-600PM).

Arrhenius plots (logarithmic plots of relaxation time against reciprocal absolute temperature) were obtained for 38, 42, 45, and 50% PVME–water systems at temperatures between –105 and –13 °C. The relaxation time,  $\tau$ , is defined by the relation,  $\tau = 1/2\pi f_{\max}$ , where  $f_{\max}$  is the peak frequency in the dielectric loss spectrum. The dielectric loss spectra for PVME–water

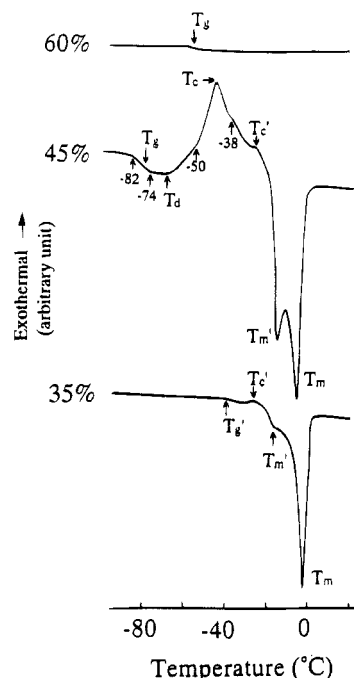


**Figure 1.** DSC curves for 35, 45, and 60% PVME–water systems at temperatures between –100 and +20 °C (The symbol  $T_d$  signifies a beginning temperature of the exotherm, and other symbols are denoted in the figure caption of Figure 2.)

systems were determined at frequencies between 10 and  $10^5$  Hz and temperatures between –100 and –15 °C.

Dielectric constants,  $\epsilon'$ , at a constant frequency of 110 Hz were measured for 30 and 45% PVME, using a heating rate of 3 °C/min between –150 and –10 °C. (The dielectric measurement method has been described previously.<sup>10,11</sup>)

Thermograms of DSC for PVME–water systems were obtained at temperatures between –100 and +20 °C and at a heating rate of 3 °C/min.

**(3) Results and Discussion. Calorimetric Behavior of PVME–Water Systems.** On heating an exothermic peak ( $T_c$ ) appears at –46 °C in the 45% PVME system as shown in Figure 1 (although it disappeared when rewarmed to –10 °C). Similar exothermic peaks have been observed in many aqueous macromolecules, and they have been attributed to the cold crystallization.<sup>12</sup> In addition, another small exothermic peak ( $T_c'$ ) is observed at –24 °C, also suggesting another recrystallization of water, as described in more detail in sections 4.iii and 4.iv. For 35% PVME, the exothermic peak ( $T_c'$ ) was also observed at –24 °C, only when rapidly cooled (at a cooling rate of 100 °C/min) (Figure 1).

An endothermic peak ( $T_m$ ) is observed just below 0 °C in each of the 35 and 45% PVME systems (Figure 1), which is obviously due to ice (free water) melting.

Another endothermic peak ( $T_m'$ ) appears at –14 °C for each curve of 35 and 45% PVME (Figure 1). However, the peak is not observed at high PVME (or low water) concentrations, at least above 60% PVME (Figure 1), indicating that the generation of this peak requires a minimum concentration of water to be present in the system. The onset of glass transition of PVME is observed at approximately –27 °C (at 100% PVME in Figure 2). From these results, it can be deduced that the endotherm at –14 °C ( $T_m'$ ) is not due to the polymer itself but due to water in the PVME–

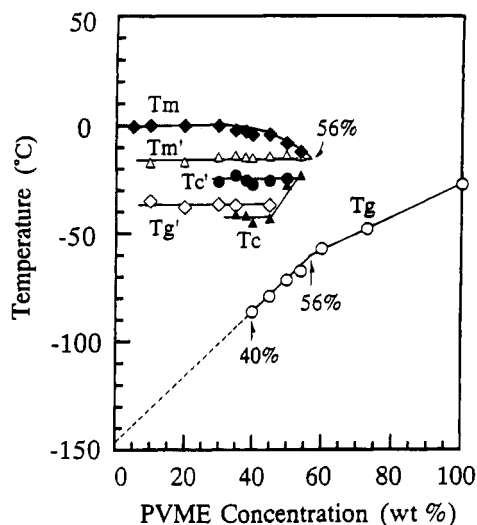


**Figure 2.** Phase diagram for PVME-water systems at subzero temperatures.  $T_m$  and  $T_m'$  are the peak temperatures of melting,  $T_c$  and  $T_c'$  are the peak temperatures of recrystallization,  $T_g$  is the glass transition temperature, and  $T_g'$  is the starting temperature of another glass transition. The interpolated broken line on the  $T_g$  curve intersects at  $-145^\circ\text{C}$ , indicating the glass transition temperature of pure liquid.

water systems (see sections 4.iii and 4.iv). We have recently determined two distinct hydration numbers for PVME, suggesting the existence of a polymer-water complex.<sup>9</sup>

Glass transition ( $T_g$ ) occurs between  $-82$  and  $-74^\circ\text{C}$  in the DSC curve of the 45% PVME system (Figure 1). The glass transition of pure water is known to take place around  $-140^\circ\text{C}$ ,<sup>13-15</sup> thus suggesting that the  $T_g$  of water in this system is altered by the presence of the polymer chains. In fact, a temperature of  $-145^\circ\text{C}$  is obtained as the  $T_g$  of pure water by extrapolating the  $T_g$  curve to zero for PVME concentration (Figure 2). Such glass transition around  $-80^\circ\text{C}$  ( $T_g$ ) and subsequent recrystallization around  $-46^\circ\text{C}$  ( $T_c$ ) are not observed in the 35% PVME system (although two endotherms  $T_m$  and  $T_m'$  are still observed). This indicates that the 35% PVME system crystallizes during cooling without forming any glass.

The transition temperatures ( $T_m$ ,  $T_m'$ ,  $T_c$ ,  $T_c'$ ,  $T_g$ , and  $T_g'$ ) depend on PVME concentration, as summarized in Figure 2. In the figure, the  $T_m$  curve ends at a PVME concentration of 56%, which signifies the concentration above which no melting transition can be observed. In addition, the  $T_g$  curve deflects at the concentration of 56% and ends at 40% (Figure 2). These two characteristic concentrations (40 and 56%) are in good agreement with those obtained from the DSC data around the cloud-point temperature given in a previous paper.<sup>9</sup> (The temperature  $T_g'$  is defined as the starting temperature of glass transition occurring in a concentrated polymer phase (see section 4.iii).

**(4) Determination of Characteristic Temperature Regions and Anomalous Dielectric Behaviors in PVME-Water Systems.** (i) **Glassy Solid Region (below  $-80^\circ\text{C}$ ).** A glassy solid state is observed at temperatures below  $-82^\circ\text{C}$  in the DSC curve for 45% PVME (Figure 1). The same temperature region (denoted by I in Table 1) is also observed below  $-79^\circ\text{C}$  in the Arrhenius curve of dielectric relaxation times,  $\tau$ , for the systems (Figure 3).

The Arrhenius curves (for 42, 45, and 50% PVME) are nonlinear in this region and can be approximately

**Table 1. Characteristic Temperature Regions for PVME-Water Systems Determined with Calorimetric, Dielectric ( $\epsilon'$  and Arrhenius Curves for Relaxation Times,  $\tau$ ), and Optical Microscopic Analyses<sup>a</sup>**

		Temperature ( $^\circ\text{C}$ )				
		-80	-60	-40	-20	0
DSC	35				exo.	endo.
	45	g.s.	II' g.t.	II''	exothermic region	endo. region
$\epsilon'$	30	I'			IV	V
	45	I	II	III		
Arr.C.	38	I'			IV	V
	45	I	II	III		
OM	30	transparent			opq	melting
	50	transparent		Spherulites	IS	AT melting Trans-parent

<sup>a</sup> The numbers, 30, 35, 38, 45, and 50 denote PVME concentrations. The broken lines denote characteristic temperatures in each region. g.s.: glass solid state. g.t.: glass transition region. exo. (endo.): exothermic (endothermic) region.  $\epsilon'$ : dielectric constant. Arr.C.: Arrhenius curve for dielectric relaxation times. OM: optical microscope observation. IS: intermediate stage of crystallization. AT: alder-twig-like crystallized water. opq: opaque.

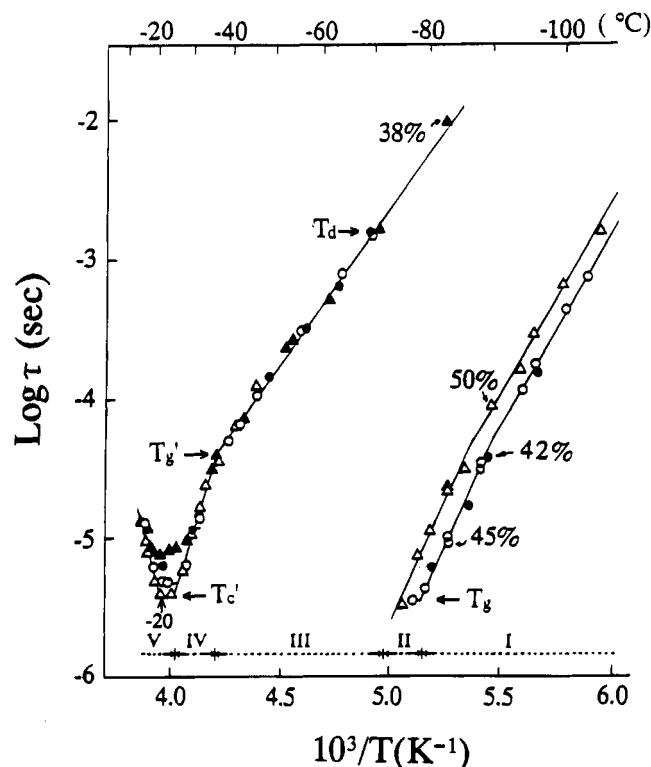


**Figure 3.** Arrhenius curves for dielectric relaxation times,  $\tau$ , for 38, 42, 45, and 50% PVME-water systems at temperatures between  $-110$  and  $-13^\circ\text{C}$ .

fit with two straight lines having different slopes. In each Arrhenius curve, the slopes correspond to activation enthalpies of 11 and 18 kcal/mol, respectively, and hence the average enthalpy is 14.5 kcal/mol. As the activation enthalpy of ice is 13 kcal/mol<sup>16</sup> and that of pure water is 5 kcal/mol,<sup>17</sup> the average enthalpy indicates that the PVME-water system is in a solid state in region I.

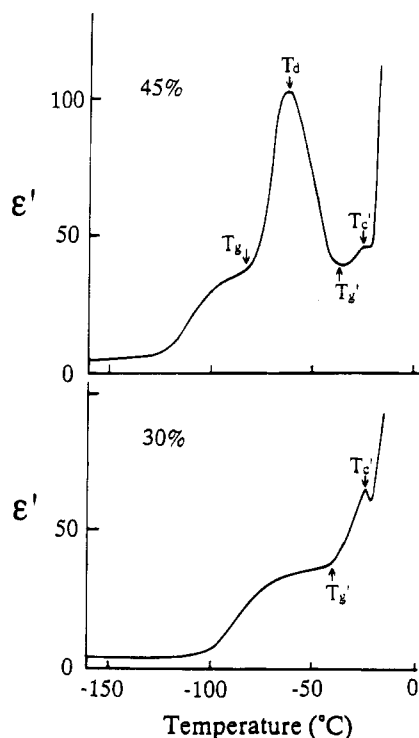


**Figure 4.** Temperature dependence of dielectric constants for 35 and 45% PVME–water systems

The characteristic temperature of  $-80^{\circ}\text{C}$  is also observed in the dielectric curve for 45% PVME (Figure 4); at this point,  $\epsilon'$  starts to rise steeply. (Another rise of  $\epsilon'$  around  $-125^{\circ}\text{C}$  is due to the relaxation of water in the glassy solid state.)

**(ii) Glass Transition Region and Mobile Region of Water ( $-80$  to  $-66^{\circ}\text{C}$ ).** A characteristic temperature region between  $-80$  and  $-66^{\circ}\text{C}$  (region II) is observed in the dielectric curve for 45% PVME (Figure 4); in this region  $\epsilon'$  rises sharply with increasing temperature. In the DSC curve for 45% PVME (Figure 1), the same temperature region (from  $-82$  to  $-66^{\circ}\text{C}$ ) can be further divided into two segments: one from  $-82$  to  $-72^{\circ}\text{C}$  (region II') and the other from  $-72$  to  $-66^{\circ}\text{C}$  (region II''). In region II', an endothermic change is observed in the 45% PVME system, which is characteristic of glass transition.

Water in this system can be expected to be mobile in both regions II' and II''. In fact,  $\epsilon'$  increases to reach a maximum value of approximately 100 for 45% PVME (Figure 4) and 360 for 50% PVME in region II (although the latter data are not shown here). This strikingly large value of  $\epsilon'$  is apparently due to an increase in ion mobility, which is induced by an increase in water mobility. Such large values of  $\epsilon'$  have been frequently observed in hydrated macromolecules with impurity ions below  $0^{\circ}\text{C}$ .<sup>18,19</sup>

**(iii) Exothermic Region Including Two Types of Recrystallization ( $-66$  to  $-20^{\circ}\text{C}$ ).** The DSC thermogram for 45% PVME shows the beginning of an exothermic heat flow at  $-66^{\circ}\text{C}$  ( $T_d$ ), a peak at  $-46^{\circ}\text{C}$  ( $T_c$ ), and shoulders at  $-50$  and  $-38^{\circ}\text{C}$  (Figure 1). The same characteristic temperatures are observed in the dielectric curve of 45% PVME (Figure 4); the dielectric constant  $\epsilon'$  begins to decrease abruptly at  $-66^{\circ}\text{C}$  and reaches a minimum at about  $-38^{\circ}\text{C}$  (region III). This drastic decrease in  $\epsilon'$  (which is opposite to the dielectric behavior in the glass transition region) suggests a sharp decrease in ion mobility and indirectly a sharp decrease

in water mobility in the system. This dielectric behavior is consistent with the onset of recrystallization in this temperature region.

There is no indication of calorimetric changes below  $-38^{\circ}\text{C}$  (region I' in Table 1) in the DSC curve for 35% PVME (Figure 1), although the exotherm  $T_c'$  and the successive endotherms  $T_m'$  and  $T_m$  are still observed. The absence of  $T_g$  (around  $-80^{\circ}\text{C}$ ) and  $T_c$  (around  $-46^{\circ}\text{C}$ ) demonstrates that the 35% PVME system crystallized during cooling.

The characteristic temperature of  $-38^{\circ}\text{C}$  is also observed (i) in the dielectric curves (Figure 4;  $\epsilon'$  begins to increase sharply at  $-38^{\circ}\text{C}$ ) and (ii) in the Arrhenius curves (Figure 3; change in slope at  $-38^{\circ}\text{C}$ ). These results indicate the onset of a transition where water becomes more mobile at  $-38^{\circ}\text{C}$  in the systems. However, this transition (together with a subsequent exotherm at  $-24^{\circ}\text{C}$  ( $T_c'$ )) was not observed in the systems rewarmed to  $-10^{\circ}\text{C}$ . This and the shape of the DSC curve around  $-38^{\circ}\text{C}$  suggest that the transition is a glass transition ( $T_g'$ ). On a cooling process, most of the water freezes, so the system will consist of a mixture of ice and a concentrated polymer solution. Thus, because the transition temperature of  $-38^{\circ}\text{C}$  is independent of initial PVME concentrations (Figure 2), the glass transition ( $T_g'$ ) is inferred to take place in the concentrated polymer phase.

The relaxation times for water in the systems are on the order of 1–10 ms (Figure 3) at the lower temperature boundary of region III in the 42, 45, and 50% PVME systems. They are approximately 1000 times larger than those for water at the higher temperature boundary of region I. This drastic change in the relaxation times indicates a decrease in the entropy of water structures in the systems. That is obvious from the definition of  $\tau$ , which is proportional to  $\exp(-\Delta S) \exp(\Delta H/kT)$ , where  $\Delta S$  and  $\Delta H$  denote the activation entropy and enthalpy, respectively,  $k$  is the Boltzmann constant, and  $T$  is the absolute temperature.

**(iv) Two Types of Water Melting ( $-20$  to  $0^{\circ}\text{C}$ ).** An anomalous relaxation process is observed in the temperature region above  $-24^{\circ}\text{C}$  (region V) in the PVME–water systems. With increasing temperature, the relaxation times change very little in the region from  $-24$  to  $-20^{\circ}\text{C}$  and then become longer (slow down) above  $-20^{\circ}\text{C}$  for each PVME concentration (Figure 3). This behavior is very curious, because in normal relaxation processes the relaxation times become shorter (faster) with increasing temperature.

To explain the slowing down of relaxation times in this region, the following can be considered as possible mechanisms: (i) a structural change in the phase of recrystallized water itself which increases the relaxation times, and (ii) the appearance and growth of another more ordered crystallized water, which has a longer relaxation time than the already recrystallized water ( $T_c$ ). In the 50% PVME systems, we actually observed the appearance of water spherulites around  $-50^{\circ}\text{C}$  (Figure 5a) and of subsequent crystallized water like an alder twig on the spherulites at  $-20^{\circ}\text{C}$  (through an intermediate stage of crystallization at temperatures between  $-27$  and  $-20^{\circ}\text{C}$ ) (Figure 5b) with an optical microscope. In the 30% PVME system, a transition also appears at  $-24^{\circ}\text{C}$ , which reflects a sudden change in the optical images from transparent to opaque, suggesting the appearance and growth of water crystallites. Thus, these data support mechanism ii. An abrupt reduction in  $\epsilon'$  at  $-24^{\circ}\text{C}$  (Figure 4) is obviously related

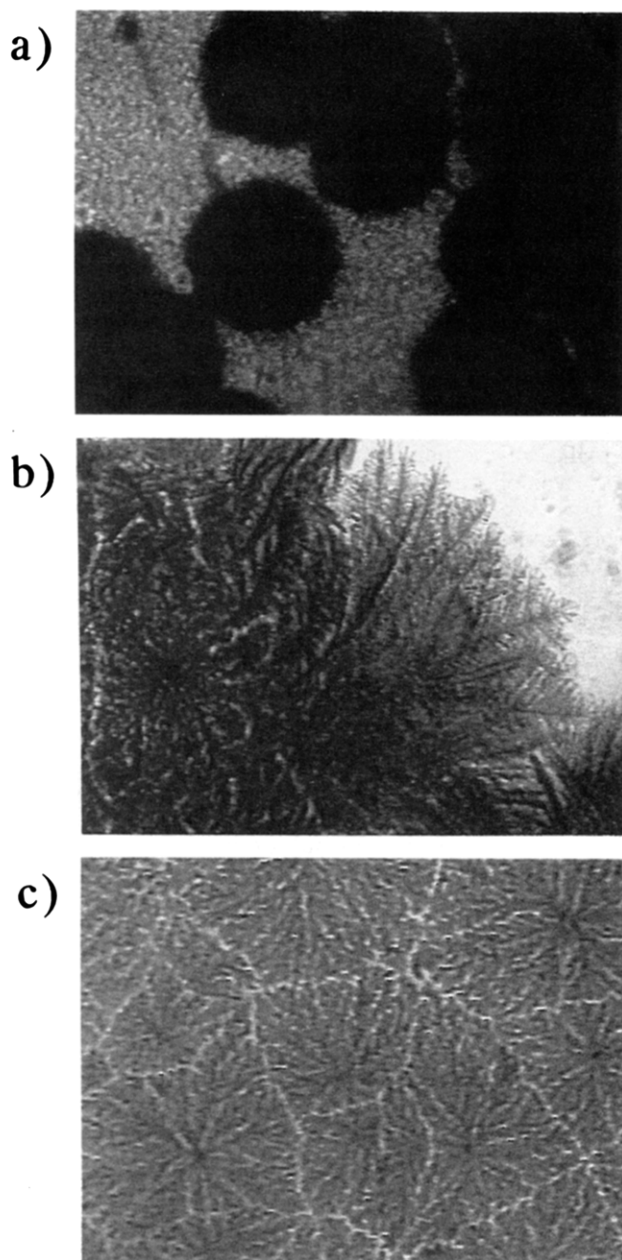


**Figure 5.** (a) Spherulites of water (black disks) at  $-34\text{ }^{\circ}\text{C}$ , (b) alder-twig-like crystallized water on the spherulites (a black spot seen at the middle of the left side of this picture is the nuclei of the spherulite) which are melting, as observed at  $-12\text{ }^{\circ}\text{C}$ , and (c) clear boundaries between spherulites at  $-19\text{ }^{\circ}\text{C}$ , in 50% PVME-water systems.

to the appearance of recrystallization at  $-24\text{ }^{\circ}\text{C}$ . On the other hand, a sudden increase in  $\epsilon'$  appears at  $-20\text{ }^{\circ}\text{C}$  (Figure 4), indicating a sharp increase in ion mobility and indirectly a sharp increase in water mobility. This is consistent with the onset of an endotherm indicating melting at  $-20\text{ }^{\circ}\text{C}$  (Figure 1) and the appearance of clear boundaries between spherulites at  $-20\text{ }^{\circ}\text{C}$  (Figure 5c).

The glass transition  $T_g$  ( $-80\text{ }^{\circ}\text{C}$ ), the recrystallization  $T_c$  ( $-46\text{ }^{\circ}\text{C}$ ), and the melting  $T_m$  ( $-2\text{ }^{\circ}\text{C}$ ) can be consid-

ered as a series of thermal transitions due to free water in the systems. On the other hand, the glass transition  $T_g$  ( $-38\text{ }^{\circ}\text{C}$ ), and the recrystallization  $T_c$  ( $-24\text{ }^{\circ}\text{C}$ ), and the endotherm  $T_m'$  ( $-14\text{ }^{\circ}\text{C}$ ) must be another series of thermal transitions in the systems. Thus, the endotherm  $T_m'$  can be attributed to melting of water in the concentrated polymer phase described in section 4.iii. The polymer concentration of the phase is estimated to be 56% from the end of the  $T_m$  curve in Figure 2. (More precisely, we determined the same critical concentration by plotting the enthalpy of free water melting ( $T_m$ ) as a function of grams of water per grams of polymer in the systems.) A hydration number calculated from the critical concentration (56%) coincides well with the one required to complete a polymer-water complex (proposed in a previous paper<sup>9</sup>). Similar successive two endotherms (just below  $0\text{ }^{\circ}\text{C}$ ) have been observed in poly(ethylene oxide) (PEO)-water systems,<sup>4-7</sup> rehydrated blood plasma (BP),<sup>20</sup> and starch and gelatin gels.<sup>21</sup> In PEO-water systems,  $T_m'$  is observed at the same temperatures, about  $-22\text{ }^{\circ}\text{C}$ , independent of system composition; this is characteristic of the melting of a binary eutectic mixture. In BP systems,  $T_m'$  and  $T_m$  are observed at about  $-23$  and  $-16\text{ }^{\circ}\text{C}$ , respectively, at a water concentration of ca. 33%, while  $T_m$  disappears below 32%. In starch and gelatin gels, the melting endotherm  $T_m'$  (around  $-10\text{ }^{\circ}\text{C}$ ) has been interpreted as being due to water confined in the gel networks.<sup>21</sup> The existence of confined water is also suggested from the observation of  $T_m'$  in sephadex gels.<sup>22</sup>

## References and Notes

- (1) Mackenzie, A. P. and Rasmussen, D. In *Water Structure at the Water-Polymer Interface*; Jellinek, H. H. G., Ed.; Plenum Press: New York, 1972; p 146.
- (2) Luyet, B.; Rasmussen, D. *Biodynamica* **1967**, *10*, 137.
- (3) Franks, F. In *Water, A Comprehensive Treatise*; Franks, F., Ed.; Plenum Press, New York, 1982; Vol. 7, p 215.
- (4) Hager, S. L.; Macrury, T. B. *J. Appl. Polym.* **1980**, *25*, 1159.
- (5) Anderson, B.; Oloffson, G. *Colloid Polym. Sci.* **1987**, *265*, 318.
- (6) Graham, N. B.; Zulfigur, M.; Nuwachuku, N. E.; Rashid, A. *Polymer* **1989**, *30*, 528.
- (7) Bogdanov, B.; Mihailov, M. *J. Polym. Sci., Polym. Phys. Ed.* **1985**, *23*, 2149.
- (8) Horne, R. A.; Almeida, J. P.; Day, A. F.; Yu, N-T. *J. Colloid Interface Sci.* **1971**, *35*, 77.
- (9) Maeda, H. *J. Polym. Sci.* **1994**, *31*, 91.
- (10) Maeda, H.; Fukada, E. *Biopolymers* **1982**, *21*, 2055.
- (11) Maeda, H. *Biophys. J.* **1989**, *56*, 861.
- (12) Ahad, E. *J. Appl. Polym. Sci.* **1987**, *22*, 1665.
- (13) Sugizaki, M.; Suga, H.; Seki, S. *Bull. Chem. Soc. Jpn.* **1968**, *41*, 2591.
- (14) Angell, C. A.; Sare, E. J. *J. Chem. Phys.* **1970**, *52*, 1058.
- (15) Bruggeller, P.; Mayer, E. *Nature* **1980**, *288*, 569.
- (16) Auty, R. P.; Cole, R. H. *J. Chem. Phys.* **1952**, *20*, 1309.
- (17) Grant, E. H. *J. Chem. Phys.* **1957**, *26*, 1575.
- (18) Maeda, H.; Ebihara, S. *J. Polym. Sci., Part B* **1990**, *28*, 2385.
- (19) Maeda, H. *J. Appl. Polym. Sci.* **1991**, *42*, 3013.
- (20) Simatos, D.; Faure, E.; Bonjour, E.; Couach, M. *Cryobiology* **1975**, *12*, 202.
- (21) Ishida, N.; Kobayashi, T.; Kainuma, K. *J. Jpn. Soc. Food Sci. Technol.* **1988**, *35*, 98.
- (22) Murase, N.; Gonda, K.; Watanabe, T. *J. Phys. Chem.* **1986**, *90*, 5420.

MA950017F